

1 **Accepted publication pre-print version**

2 ***Pseudomonas putida* biofilm dynamics following a single pulse of silver nanoparticles**

3 Florian Mallevre, Teresa F. Fernandes, Thomas J. Aspray*

4 School of Life Sciences, NanoSafety Research Group, Heriot-Watt University, Edinburgh

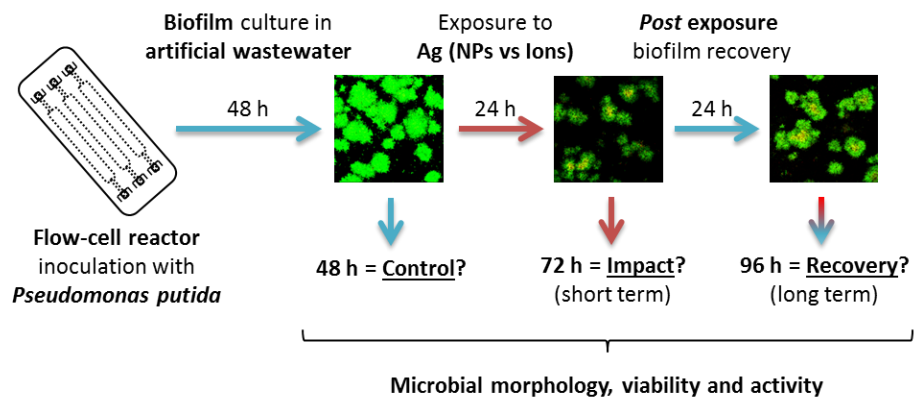
5 EH14 4AS, Scotland, UK

6 * Corresponding author. Tel.: +44 (0)131 451 3974; fax: +44 (0)131 451 3009; e-mail address:

7 T.J.Aspray@hw.ac.uk, thomasaspray@gmail.com (T. J. Aspray).

8 **Graphical abstract**

9
10
11
12
13
14
15
16



17 **Abstract**

18 *Pseudomonas putida* mono-species biofilms were exposed to silver nanoparticles (Ag NPs) in
19 artificial wastewater (AW) under hydrodynamic conditions. Specifically, 48 h old biofilms
20 received a single pulse of Ag NPs at 0, 0.01, 0.1, 1, 10 and 100 mg L⁻¹ for 24 h in confocal
21 laser scanning microscopy (CLSM) compatible flow-cells. The biofilm dynamics (in terms of
22 morphology, viability and activity) were characterised at 48, 72 and 96 h. Consistent
23 patterns were found across flow-cells and experiments at 48 h. Dose dependent impacts of
24 NPs were then shown at 72 h on biofilm morphology (*e.g.* biomass, surface area and
25 roughness) from 0.01 mg L⁻¹. The microbial viability was not altered below 10 mg L⁻¹ Ag NPs.
26 The activity (based on the D-glucose utilisation) was impacted by concentrations of Ag NPs
27 equal and superior to 10 mg L⁻¹. Partial recovery of morphology, viability and activity were
28 finally observed at 96 h. Comparatively, exposure to Ag salts resulted in *ca.* one order of
29 magnitude higher toxicity when compared to Ag NPs. Consequently, the use of a continuous
30 culture system and incorporation of a recovery stage extends the value of biofilm assays
31 beyond the standard acute toxicity assessment.

32 **Keywords**

33 Biofilm; Flow-Cell Reactor; *Pseudomonas putida*; Silver Nanoparticle; Recovery;
34 Ecotoxicology.

35 1. Introduction

36 Current interest in engineered nanoparticles (NPs) is clear given their various attractive
37 physico-chemical properties (Ju-Nam and Lead 2008; Rai *et al.*, 2014). There are
38 nevertheless legitimate concerns regarding the actual risk associated with the emergence of
39 anthropogenic NPs in the environment (Duester *et al.*, 2014; Eduok *et al.*, 2013). Reported
40 environmental concentrations of the majority of NPs in freshwater systems are in the $\mu\text{g L}^{-1}$
41 range and likely to increase due to the wide applications of NPs in societal and medical
42 products (Gottschalk *et al.*, 2013; Ju-Nam and Lead 2008; Rai *et al.*, 2014). Consequently,
43 the potential adverse effects of NPs on microorganisms in environmental systems (natural
44 and otherwise) need to be appraised.

45 Bacteria have already been used intensively in nano(eco)toxicology, especially using
46 planktonic cultures (Holden *et al.*, 2014; Kahru and Ivask, 2013). Biofilms, defined as self-
47 produced matrix enclosed mono or multi-species microbial communities that adhere to
48 biological or non-biological surfaces or interfaces (Stewart and Franklin, 2008), are
49 nonetheless referred as the main living form of bacteria in the environment (Hall-Stoodley
50 *et al.*, 2004). Structurally organized, dynamic and complex ubiquitous biological systems,
51 biofilms have in addition essential beneficial implications (*e.g.* facilitators within the natural
52 environment or in the treatment of wastewaters) (Hall-Stoodley *et al.*, 2004; Stewart and
53 Franklin, 2008). Consequently, biofilm based assays represent a desirable source of
54 information in nano(eco)toxicology.

55 Despite their relevance, only a handful of nano(eco)toxicological studies has been carried
56 out using biofilms to date. Assays performed under static conditions (*i.e.* here referred to as
57 static biofilms) using microtitre plates or glass slides, coupled with spectrophotometry or
58 confocal laser scanning microscopy (CLSM), have been reported (Choi *et al.*, 2010; Dong and
59 Yang, 2014; Dror Ehre *et al.*, 2010; Inbakandan *et al.*, 2013; Martinez-Gutierrez *et al.*, 2013;
60 Radzig *et al.*, 2013; Raftery *et al.*, 2014). However, biofilms obtained under hydrodynamic
61 conditions (*i.e.* here referred to as non-static biofilms) are fully hydrated, planktonic free
62 and mature structures compared to the static biofilms (Buckingham-Meyer *et al.*, 2007;
63 Crusz *et al.*, 2012; Weiss Nielsen *et al.*, 2011). Studies based on non-static biofilms are
64 therefore gradually emerging using diverse rotating biological contactor and reactors

65 (Fabrega *et al.*, 2009; Hou *et al.*, 2014; Martinez-Gutierrez *et al.*, 2013; Park *et al.*, 2013).
66 Unlike most reactors, the flow-cell systems present the additional advantages of real time,
67 non-invasive and non-destructive versatile studies (Crusz *et al.*, 2012; Weiss Nielsen *et al.*,
68 2011). Consequently, a high potential of assay development is associated with the use of
69 flow-cell reactors.

70 Applications of flow-cell reactors were reported in (eco)toxicology for the testing of silver
71 sulfadiazine and solvent styrene on *Pseudomonas* spp. biofilms (Bjarnsholt *et al.*, 2007;
72 Halan *et al.*, 2011). Examples in nano(eco)toxicology are particularly scarce at the present
73 time as the sole contribution is the study by Fabrega *et al.* (2009) where the interactions
74 between Ag NPs and *Pseudomonas putida* biofilms were investigated (*e.g.* accumulation and
75 uptake of NPs). These authors especially stressed the need of complementary studies
76 dedicated to the assessment of long term effects (*i.e.* including recovery) of NPs to complex
77 materials such as biofilms. This was further emphasised in recent literature (Handy *et al.*,
78 2012) as an area not being considered in most of the nano(eco)toxicological studies
79 published so far.

80 The present study builds on these pioneer examples (Bjarnsholt *et al.*, 2007; Fabrega *et al.*,
81 2009; Halan *et al.*, 2011) and aims to assess the temporal impact following a single pulse of
82 NPs on non-static mono-species biofilm morphology, viability and activity using flow-cell
83 reactors. Silver (Ag) is prioritised given that it is a well-known bactericidal agent and one of
84 the most widely used NPs in a large range of applications (Morones *et al.*, 2005; Rai *et al.*,
85 2014). *P. putida* based biofilms are considered since they are used with flow-cell reactors
86 and are commonly proposed as an environmental bacterial model (Bjarnsholt *et al.*, 2007;
87 Fabrega *et al.*, 2009; Halan *et al.*, 2011). Consequently, the dynamics (considering the
88 impact in the short term as well as the potential recovery in the long term) of mature *P.*
89 *putida* biofilms (considering morphology, viability and activity) in response to a single pulse
90 of Ag NPs and salts are here reported and discussed.

91 **2. Material and methods**

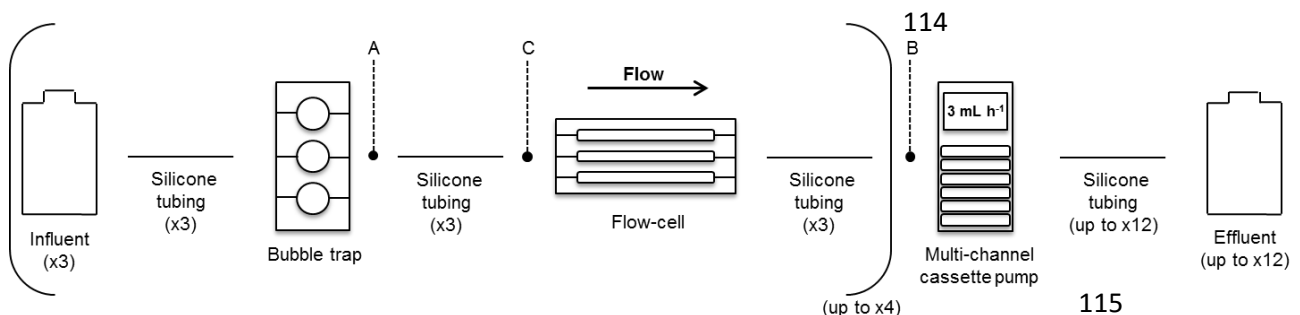
92 2.1. Material

93 The biofilm reactor consisted of inverted Perspex flow-cells (CLSM compatible) and bubble
 94 traps purchased from DTU Systems Biology (Lyngby, Denmark) used in combination with 24
 95 x 50 mm glass coverslips (1.5 mm thick) from SLS UK Ltd and silicone (Versilic) and Marprene
 96 (Watson Marlow UK Ltd) tubings as reported previously (Crusz *et al.*, 2012; Weiss Nielsen *et*
 97 *al.*, 2011). Representative Ag NPs (*i.e.* JRCNM03000a also named Ag NM-300K NPs, which
 98 are negatively charged nanoparticles with a primary size *ca.* 15 nm delivered in suspension
 99 at 10 % (w/v) in 4 % (v/v) each of polyoxyethylene glycerol trioleate and polyoxyethylene
 100 (20) sorbitan mono-laurat) were obtained from the European Commission's Joint Research
 101 Centre (Ispra, Italy) and characterised previously (Klein *et al.*, 2011; Mallevre *et al.*, 2014).
 102 The Filmtracer Live/Dead[®] Biofilm Viability Kit was purchased from Life Technologies UK Ltd.
 103 D-glucose, silver nitrate (AgNO₃), phenol and sulphuric acid were from Fisher Scientific UK
 104 Ltd. Rely⁺On Virkon[®] disinfectant was from DuPont. A silver single element standard was
 105 purchased from Perkin Elmer UK Inc.

106 2.2. Methods

107 2.2.1. Culture of *P. putida* mono-species biofilms in a flow-cell reactor

108 Biofilms were cultured under hydrodynamic (laminar) conditions using parallelised flow-cells
 109 as schematised in Figure 1. Wastewater isolated *Pseudomonas putida* BS566::*luxCDABE*
 110 (hereafter referred to as *P. putida* BS566) (Wiles *et al.*, 2003) was used as a model
 111 bacterium for establishing mono-species biofilms. All experiments were performed in
 112 artificial wastewater (AW), the composition of which is reported elsewhere (Mallevre *et al.*,
 113 2014) using D-glucose at 0.5 % (w/v) as sole carbon source.



116 **Fig. 1: Schematic diagram of the set up reactor.** The reactor comprised parallelised CLSM
 117 compatible flow-cells (bearing independent channels) complying with the above presented

118 configuration. A, B and C refer to key actions performed during the inoculation process: clamp off in
119 A, dis-connect in B then inoculate in C.

120 The set up reactor was cleaned with Virkon[®] 1 % (w/v) then extensively washed with sterile
121 deionised water at 15 mL channel⁻¹ h⁻¹ using a 205U multi-channel cassette pump (Watson
122 Marlow UK Ltd). The channels were then filled with sterile AW and left at minimal flow rate
123 overnight. Prior to the inoculation, the bacterium was pre-cultured overnight at 28 ± 2 °C
124 under shaking conditions (140 rpm) in AW then diluted in order to reach a final
125 concentration *ca.* 10⁷ CFU mL⁻¹ (corresponding to a dilution about 1:100e). Each channel was
126 then independently inoculated with 200 µL of freshly prepared cell suspension by: clamping
127 off the tubing upstream of each flow-cell (Fig. 1, position A), disconnecting the tubing
128 downstream of the flow-cells (Fig. 1, position B) and injecting the bacterial suspension
129 within the channels (Fig. 1, position C). After inoculation, the tubings were re-connected and
130 dis-clamped; the flow-cells were then incubated 1 h (*i.e.* flow off, glass coverslip on bottom).
131 The biofilms were cultured (*i.e.* glass coverslip on top) for 48 h in AW with a consistent flow
132 rate of 3 mL channel⁻¹ h⁻¹.

133 2.2.2. Experimental scenario of culture, exposure and recovery

134 Stock suspensions of Ag NPs at 100 mg L⁻¹ were freshly prepared in AW prior to each
135 experiment, sonicated (2 x 8 min in a Kerry ultrasonic water bath at 38 ± 10 KHz), then
136 serially diluted to give final concentrations of 0, 0.01, 0.1, 1, 10 and 100 mg L⁻¹ applied for 24
137 h at 3 mL channel⁻¹ h⁻¹ on 48 h old biofilms. Ag ions (applied as AgNO₃) were similarly tested
138 at final concentrations of 0, 0.001, 0.01, 0.1, 1 and 10 mg L⁻¹. Virkon[®] 1 % (w/v) was tested as
139 a toxicant positive control. After exposure, upstream tubings were purged and the system
140 filled with fresh AW (*i.e.* free from any toxicant) for an additional 24 h of culture at 3 mL
141 channel⁻¹ h⁻¹. Three time points were defined: 48 h (*i.e.* assessing the biofilm establishment
142 and culture), 72 h (*i.e.* assessing the short term effects of the exposure) and 96 h (*i.e.*
143 assessing the long term effects of the exposure and the potential recovery of the biofilms).

144 2.2.3. Biofilm morphology, viability and activity characterisation

145 Morphology and viability of the biofilms were characterised within the flow-cells at 48, 72
146 and 96 h by CLSM in a non-destructive manner. Image capture was performed on a Leica

147 Microsystems TCS SP2 inverted CLSM with a HCX APO CS 63x 1.4 oil immersion lens after
148 staining with the Filmtracer Live/Dead® Biofilm Viability Kit following recommendations of
149 the manufacturer. Both Syto® 9 (green, characterising the live cells) and Propidium Iodide
150 (PI, red, characterising the dead cells) stains were excited with a laser source at 488 nm in a
151 unidirectional mode at speed of 400 Hz. Emissions were simultaneously monitored *via*
152 distinct photomultipliers set at 510 - 530 nm and 610 - 630 nm, respectively. A total of seven
153 z-stacks (characterised by 100 images at 512 x 512 in resolution in a consistent 100 µm
154 thickness window) were randomly registered *per* condition (*i.e. per* channel) for each time
155 point in all experiments. CLSM images were processed by the Leica Microsystems LAS AF
156 Lite software for viability and analysed with the COMSTAT 1 program (Danish Technical
157 University) using Matlab R2013b (MathWorks, USA) software for morphology (*e.g.* total
158 biomass, maximum thickness, mean thickness, roughness coefficient and surface area) as
159 described in Heydorn *et al.* (2000). Data from the COMSTAT based analysis were further
160 processed following:

161
$$\text{Relative evolution (in \% terms)} = (\text{results at } y - \text{results at } x) / (\text{results at } x) \quad \text{eq. 1}$$

162 where x, y are 48 and 72 h or 72 and 96 h, respectively.

163 The microbial activity was assessed by the monitoring of the D-glucose utilisation (*i.e.* sole
164 carbon source) within the experimental scenario. The amount of D-glucose was quantified in
165 both influent and effluent collected samples at 48, 72 and 96 h (after filtration at 0.2 µm)
166 following the phenol-sulphuric acid assay based protocol described elsewhere (Fournier,
167 2001). Then the percentage of D-glucose remaining in effluents (hereafter referred to as D-
168 glucose ratio) was calculated for each condition and time point.

169 2.2.4. Nanoparticle characterisation

170 The Ag NPs were analysed by UV-Visible spectrophotometry (UV-Vis) using an Evolution 600
171 spectrophotometer (Fisher Scientific, UK) and by Dynamic Light Scattering (DLS) using a
172 Nanosizer (Malvern, UK) as described in Mallevre *et al.* (2014) in influent and effluent
173 collected samples at 48, 72 and 96 h (after filtration at 0.2 µm). The concentration of total
174 silver element was measured in collected samples by Atomic Absorption Spectroscopy (AAS)
175 using an AAnalyst 200 Spectrometer (Perkin Elmer, UK) calibrated with an Ag single element

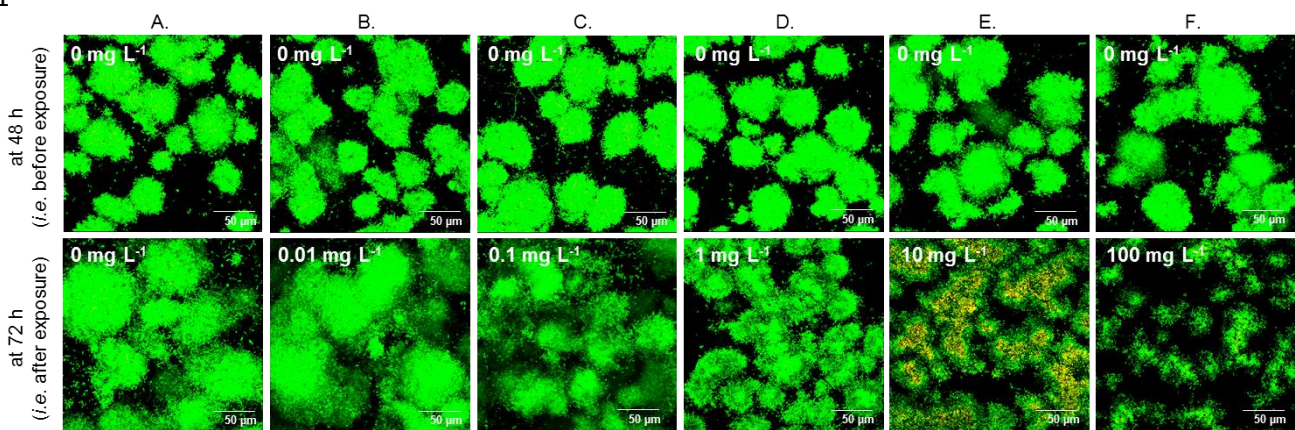
176 standard at concentrations of 0.156, 0.312, 0.625, 1.25, 2.5 and 5 mg L⁻¹ (R² = 0.9986 ±
177 0.0004, n = 4). The size distribution (z-average) and zeta potential data were treated with
178 the Zetasizer software (Malvern, UK).

179 3. Results

180 3.1. Characterisation of the *P. putida* control biofilms at 48 h

181 Representative examples of CLSM z-stack obtained *ante* exposure are presented in Figure 2
182 (top row). *P. putida* BS566 formed distinct and consistent microcolonies in D-glucose
183 supplemented AW across channels. This was confirmed across experiments as well *via* the
184 morphology related information obtained by the COMSTAT based analysis. Specifically
185 (considering 210 z-stacks in total with n = 5), control biofilms at 48 h were consistently
186 characterised by comparable biomass, maximum and mean thickness, roughness and
187 surface area of: 27.5 ± 2.6 μm³ μm⁻², 94.4 ± 3 μm, 50.2 ± 2.8 μm, 0.48 ± 0.01 and 3.2 ± 0.1
188 10⁶ μm², respectively. No red staining (*i.e.* dead cells) was observed. From a microbial
189 activity standpoint (Fig. 3), *ca.* 70 % of the original D-glucose loading was consistently found
190 in the effluents across channels and experiments.

191



192 **Fig. 2: Qualitative characterisation of the biofilm morphology *ante* and *post* exposure to Ag NPs.** *P.*
193 *putida* biofilms were cultured for 48 h then exposed to 0, 0.01, 0.1, 1, 10 and 100 mg L⁻¹ Ag NPs for
194 24 h (from A to F, respectively). Biofilms were analysed by CLSM after live/dead staining at 48 h (*i.e.*
195 *ante* exposure, top row) and at 72 h (*i.e. post* exposure, bottom row). Representative examples of
196 maximised z-stack are shown. Each image represents 1 out of 7 z-stacks randomly registered *per*

197 condition for 1 experiment. Additional examples of result at 72 h from the replicate experiments (n =
198 5) are presented in the supplementary material (Fig. S1). Scale is 50 μm wide.

199 3.2. Characterisation of the *P. putida* exposed biofilms at 72 h

200 Representative examples of CLSM z-stack registered at 72 h *post* exposure to a single pulse
201 of 0, 0.01, 0.1, 1, 10 and 100 mg L^{-1} Ag NPs for 24 h are presented in Figure 2 (bottom row).
202 Additional examples are provided in the supplementary material (Fig. S1).

203 From a morphological viewpoint, larger and less discrete microcolonies were observed at 72
204 h than at 48 h for the control (Fig. 2, column A). Biofilms exposed to 0.01 mg L^{-1} Ag NPs
205 showed comparable development overall (Fig. 2, column B). However the biofilm
206 development was visibly altered at 0.1 mg L^{-1} ; dose dependent impacts of Ag NPs were then
207 observed with, finally, sparsely distributed residues of microcolonies characterised at 100
208 mg L^{-1} (Fig. 2, columns C - E). Red staining was obtained (in 3 out of 5 experiments) at 10 mg L^{-1}
209 L^{-1} exclusively.

210

211

212

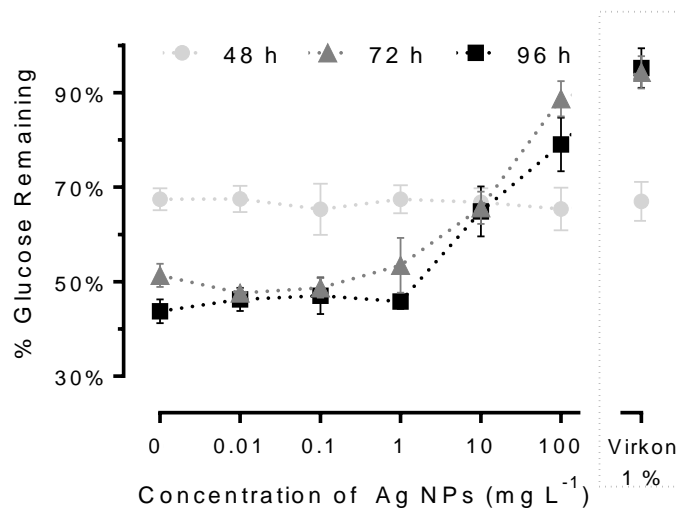
213

214

215

216

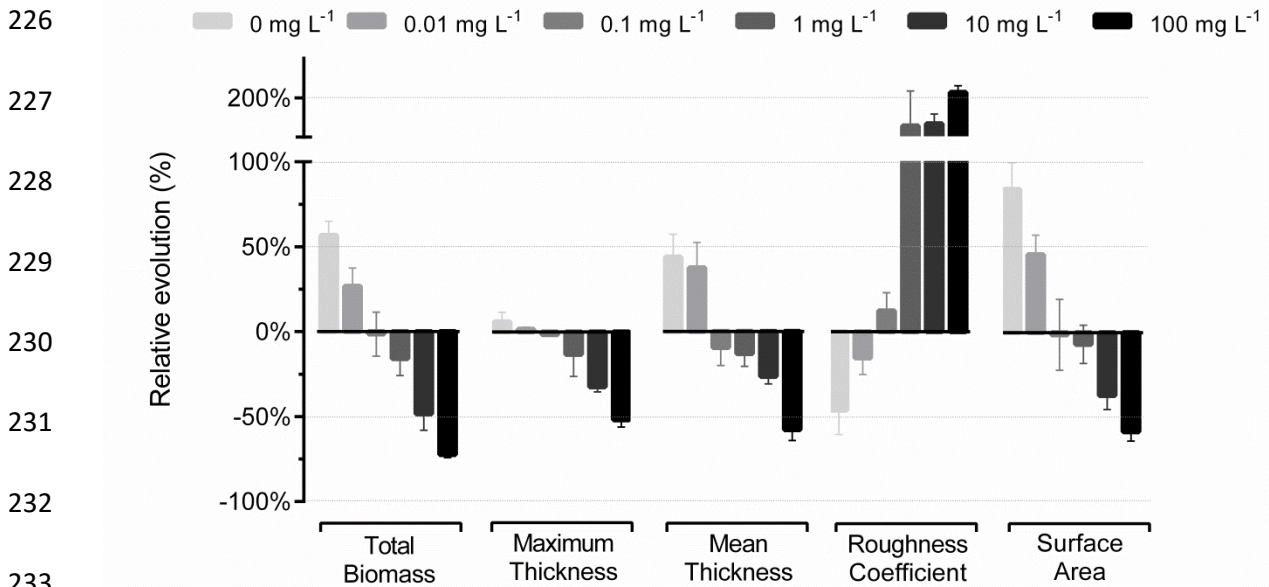
217



218 **Fig. 3: Quantitative characterisation of the microbial activity (Ag NP case).** Samples collected
219 upstream (*i.e.* in influents) and downstream (*i.e.* in effluents) of the flow-cells at 48, 72 and 96 h
220 were used for D-glucose quantification *via* the phenol - sulphuric acid assay. Presented data are
221 mean \pm SEM (n = 4) of the calculated D-glucose remaining (in % terms) in effluents *per* tested
222 condition. Corresponding results for the Ag ion case are shown in Figure S3. The detailed findings

223 from the statistical analysis *via* multiple t-tests (corrected with the Holm-Sidak method) considering
224 two parameters at a time are shown in the supplementary material (Fig. S4).

225



234 **Fig. 4: Quantitative characterisation of the biofilm morphology *post* exposure to Ag NPs.**

235 Histogram of the relative evolution (in % terms) of the descriptive biofilms parameters (*e.g.* total
236 biomass, maximum thickness, mean thickness, roughness and surface area) *post* exposure for 24 h
237 to Ag NPs at 0, 0.01, 0.1, 1, 10 and 100 mg L⁻¹ is presented. Data, calculated *per* channel as (results at
238 72 h - results at 48 h) / (results at 48 h) after the COMSTAT analysis of the registered z-stacks, are
239 mean ± SEM (n = 5). For each experiment 7 z-stacks were analysed *per* channel (*i.e.* *per* condition) at
240 both time points.

241

242 The corresponding information from the COMSTAT analysis is shown in Figure 4. Overall
243 results confirmed the dose dependent impact of Ag NPs on biofilm morphology following a
244 24 h pulse. The trend was characterised by a decrease in total biomass, thickness, surface
245 area and an increase in roughness with increasing concentrations of NPs. More specifically,
246 non-exposed biofilms gained 57 ± 8 % of biomass in 24 h; meanwhile the 0.01 mg L⁻¹
247 exposed biofilms gained significantly less (27 ± 11 %) (as determined *via* multiple t-tests
248 using the Holm-Sidak method, reporting significance with *p* value < 0.05). The altered
249 evolution of both the roughness and surface area related information was correlatively

250 observed at 0.01 mg L⁻¹ compared to the non-exposed biofilms. Impact on thickness was not
251 evident at 0.01 mg L⁻¹ though. Comparatively at 0.1 mg L⁻¹ Ag NPs, evident impacts on
252 biomass, roughness, surface area and mean thickness were observed compared to the
253 control; according to the COMSTAT results *post* exposure biofilms were *in fine* rather similar
254 to biofilms characterised *ante* exposure. The next concentrations of 1, 10 and 100 mg L⁻¹ led
255 to consistent dose dependent results with detrimental effects at 100 mg L⁻¹ resulting in *ca.*
256 75 % of the biomass and *ca.* 50 % of the thickness and surface area being lost when
257 compared to the respective biofilm characteristics before exposure. Similarly, the roughness
258 was increased by more than 200 % whereas non-exposed biofilms had their roughness
259 decreased by *ca.* 50 % for the same 24 h period.

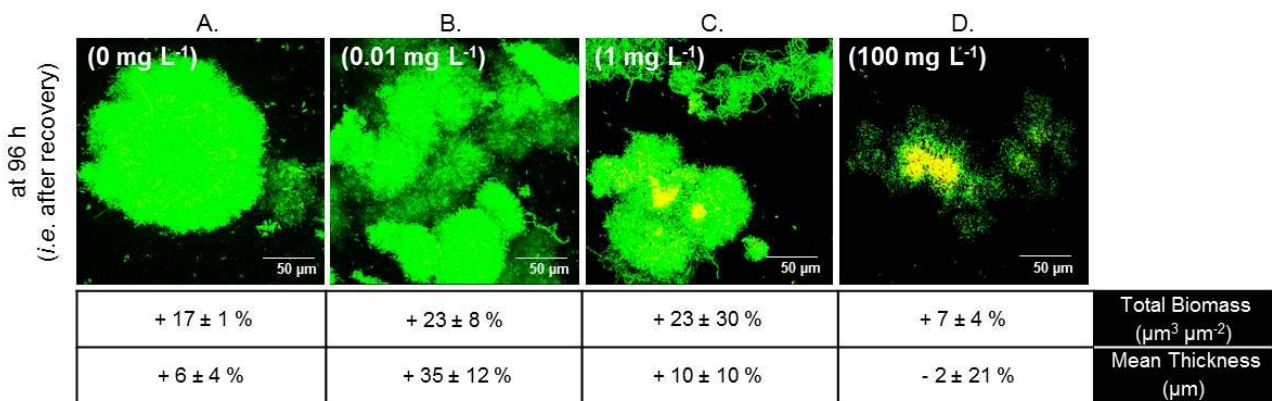
260 Regarding the microbial activity, comparable amounts of D-glucose (*ca.* 50 % of the original
261 loading) were found in effluents at 72 h *post* exposure to 0, 0.01 and 0.1 mg L⁻¹ Ag NPs (Fig.
262 3). Results were found significantly different (*i.e.* lower D- glucose ratios, increased activity)
263 compared to results at 48 h. Percentages of remaining D-glucose between 90 % and 100 %
264 were obtained *post* exposure to 100 mg L⁻¹ Ag NPs and Virkon® 1 %; results which were
265 found significantly different from data at 48 h with the same channels and from data at 72 h
266 with the other channels. Results obtained *post* exposure to 10 mg L⁻¹ (*ca.* 70 % of the
267 original loading) were non-significantly different to those obtained at 48 h. The intermediate
268 concentration of 1 mg L⁻¹ showed the largest SEM of the 72 h data with D-glucose ratios
269 varying between 45 % and 60 %; results which were found significantly different from data
270 at 48 h but not from 0.1 mg L⁻¹ and 10 mg L⁻¹ related data at 72 h.

271 Parallel experiments were performed with Ag ions at 0, 0.001, 0.01, 0.1, 1 and 10 mg L⁻¹ (n =
272 3). Comparable dose dependent toxicity patterns were observed overall on morphology (Fig.
273 S2, top row) and activity (Fig. S3) but shifted by at least one order of magnitude, the Ag ions
274 being more toxic than the tested Ag NPs. Red staining (*i.e.* dead cells) occurred consistently
275 after exposure to 1 and 10 mg L⁻¹. No biofilms were visible at 72 h after exposure to Virkon®
276 1 % (data not shown) as a positive control. Exposure to Ag NM-300K NP dispersant only has
277 already been shown not to be toxic *per se* to *P. putida* elsewhere (Malleuvre *et al.*, 2014).

278 3.3. Characterisation of the *P. putida* recovering biofilms at 96 h

279 Biofilms were left to recover for 24 h in AW *post* exposure. Examples of characteristic CLSM
 280 z-stack registered at 96 h for selected conditions (0, 0.01, 1 and 100 mg L⁻¹) along with the
 281 relative evolution (in % terms) of selected descriptive parameters (total biomass and mean
 282 thickness) are presented in Figure 5. Additional examples of CLSM result from replicate
 283 experiments are proposed in the supplementary material (Fig. S4).

284 From a morphological viewpoint (Fig. 5 A), the non-exposed biofilms were found to have
 285 developed, gaining more than 15 % in biomass and 6 % in mean thickness compared to
 286 results at 72 h. Comparatively, the exposed biofilms showed various patterns at 96 h as they
 287 were clearly recovering at 0.01 mg L⁻¹ (+23 ± 8 % in biomass and +35 ± 12 % in mean
 288 thickness, no dual staining; Fig. 5 B) and struggling for survival at 100 mg L⁻¹ (+7 ± 4 % in
 289 biomass and -2 ± 21 % in mean thickness, dual staining; Fig. 5 D). Very variable results across
 290 experiments were obtained at 1 mg L⁻¹ with evolutions in biomass and mean thickness up to
 291 +50 % and +20 % or down to -10 % and 0 %, respectively (Fig. 5 C). Dual staining as well as
 292 possibly re-structuring microcolonies (*i.e.* presence of filaments) were also reported at 1 mg
 293 L⁻¹. Tested 0.1 and 10 mg L⁻¹ concentrations led to similar dose dependent results (Fig. S5).
 294



295 **Fig. 5: Biofilm morphology recovery assessment.** Representative examples of maximised z-stack
 296 registered at 96 h following the recovery period after exposure to 0 (A), 0.01 (B), 1 (C) and 100 mg L⁻¹
 297 (D) Ag NPs are shown. Each image represents 1 out of 7 z-stacks registered *per* condition for 1
 298 experiment. Results following other tested concentrations of Ag NPs (0.1 and 10 mg L⁻¹) as well as
 299 additional examples of result for replicate experiments (n = 3) are presented in the supplementary
 300 material (Fig. S5). Scale is 50 μm wide. The corresponding relative evolution (in % terms, according
 301 to *eq. 1*) in total biomass and mean thickness calculated between 72 and 96 h is also presented.

302 Regarding the microbial activity (Fig. 3), comparable D-glucose ratios close to 45 % were
303 observed at 96 h from 0 mg L⁻¹ to 1 mg L⁻¹ tested NP concentrations. Significantly higher
304 ratios *ca.* 70 % and 80 % (*i.e.* decreased microbial activity) were obtained for 10 and 100 mg
305 L⁻¹ Ag NPs. Overall results at 96 h were not found significantly different compared to
306 percentages of D-glucose remaining calculated at 72 h (Fig. S4) but they were found
307 significantly different (up to 1 mg L⁻¹) compared to results obtained at 48 h.

308 Experiments with Ag ions at 0, 0.001, 0.01, 0.1, 1 and 10 mg L⁻¹ led to more efficient
309 recovery patterns (n = 3) (Fig. S2, bottom row; Fig. S3; Fig. S4). Overall results at 96 h were
310 found significantly different (up to 1 mg L⁻¹) from the ratios calculated at 72 h (Fig. S4). No
311 biofilms were visible at 96 h *post* exposure to Virkon® 1 % (data not shown); percentages of
312 D-glucose remaining in effluents were found consistently *ca.* 95 % of the original loading
313 (Fig. 3).

314 3.4. Characterisation of Ag NPs within the experimental scenario

315 Ag NPs were characterised by DLS and UV-Vis after sampling upstream (*i.e.* in influents) and
316 downstream (*i.e.* in effluents) of the flow-cells at 48, 72 and 96 h. As shown in Figure 6 A,
317 UV-Vis spectra of Ag NPs, characterised by a sole peak *ca.* 413 nm (0.9 a.u.), were
318 comparable at the beginning and at the end of the 24 h exposure period upstream of the
319 flow-cells. In downstream samples: no peak was observed at 48 h, non-comparable profiles
320 characterised by a sole peak *ca.* 415 nm (0.4 a.u.) were then obtained at 72 h. No specific
321 peak was registered at 96 h regardless of the sample. As shown in Figure 6 B, comparable
322 hydrodynamic size and zeta potential data were obtained by DLS at both 48 and 72 h in
323 upstream samples: 51 ± 1.4 nm and -4.8 ± 0.8 mV, 46.7 ± 2.8 nm and -3.1 ± 1 mV,
324 respectively. In downstream samples, hydrodynamic size and zeta potential results of 155.2
325 ± 14.6 nm and -12.9 ± 0.5 mV were respectively obtained at 72 h; 48 h samples were not
326 suitable for DLS analysis (*i.e.* due to the absence of NPs). Results at 72 h were found
327 significantly different between both types of sample. Mean polydispersity index (PDI) was
328 0.46 ± 0.02. Samples from 96 h were not suitable for DLS analyses either (data not shown).

329 Ag concentrations (*i.e.* 1, 10 and 100 mg L⁻¹) were confirmed by AAS in upstream samples at
330 both 48 and 72 h. Comparatively, the respective concentrations in downstream samples

331 returned to be $69 \pm 5 \%$, $51 \pm 10 \%$ and $89 \pm 7 \%$ of the concentrations measured in
 332 upstream samples when tested at 72 h. The concentration of Ag was below the lower
 333 detection limit of the apparatus (*i.e.* $< 0.1 \text{ mg L}^{-1}$) when tested at 96 h regardless of the
 334 sample.

335

336

337

338

339

340

341

342

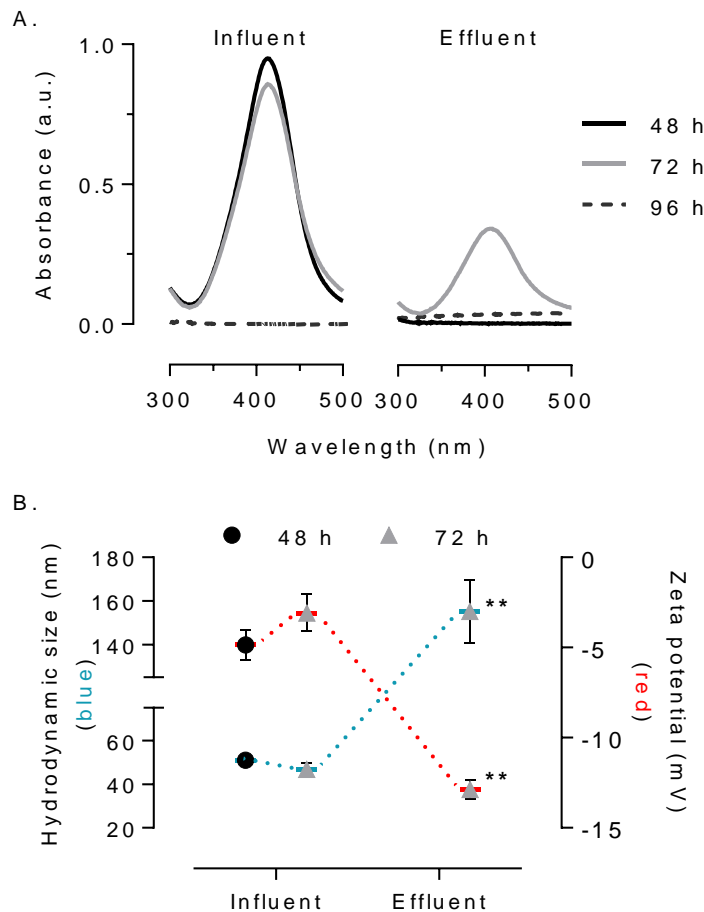
343

344

345

346

347



348 **Fig. 6: Ag NP characterisation.** Samples were collected upstream (*i.e.* in influents) and downstream
 349 (*i.e.* in effluents) of the flow-cells at 48, 72 and 96 h then characterised by DLS (A) and UV-Vis (B)
 350 when applicable. Data are mean \pm SEM ($n = 3$) when tested at 10 mg L^{-1} . Significantly different
 351 between samples *via* multiple t-tests corrected with Holm-Sidak with a p value < 0.05 (**).

352

353 4. Discussion

354 4.1. Short term effects

355 We have shown previously (Malleve *et al.*, 2014) that the tested NPs (*i.e.* Ag NM-300K
356 representative NPs from the OECD) were toxic to planktonic *P. putida* in AW with IC₅₀ values
357 *ca.* 5 mg L⁻¹ after 1 h of exposure and that Ag ions (applied as AgNO₃) were comparatively at
358 least ten times more toxic. The toxicity of Ag NPs to planktonic bacteria was mainly reported
359 in the 1 - 10 mg L⁻¹ range (Chernousova and Epple, 2013) and the frequent higher toxicity of
360 Ag ions compared to NPs was equally reported (Notter *et al.*, 2014). The toxicity of Ag NPs
361 to various static biofilms was also reported in the literature (Choi *et al.*, 2010; Dror Ehre *et*
362 *al.*, 2010; Inbakandan *et al.*, 2013; Martinez-Gutierrez *et al.*, 2013; Radzig *et al.*, 2013;
363 Raftery *et al.*, 2014). Overall conclusions emphasised that Ag NPs were harmless below 1 mg
364 L⁻¹, inhibitory in the 1 - 10 mg L⁻¹ range and lethal above 100 mg L⁻¹. The higher resistance of
365 biofilms, under hydrodynamic conditions, compared to the planktonic cells supports
366 previous findings using static biofilms (Choi *et al.*, 2010; Inbakandan *et al.*, 2013; Martinez-
367 Gutierrez *et al.*, 2013; Radzig *et al.*, 2013; Raftery *et al.*, 2014).

368 From a non-static biofilm viewpoint, there are too few studies using flow-cell reactors at the
369 present time to draw conclusive trends. Pioneer works of Bjarnsholt *et al.* (2007) showed
370 toxic effects of Ag sulfadiazine *ca.* 10 mg L⁻¹ on mature *Pseudomonas* spp. biofilms. Fabrega
371 *et al.* (2009) thereafter discussed the accumulation of Ag NPs onto and into *Pseudomonas*
372 spp. biofilms and reported the absence of impact on viability up to 2 mg L⁻¹. Correlatively
373 herein, the viability of biofilms was not visibly affected *post* exposure to a single 24 h pulse
374 of Ag NPs at 1 mg L⁻¹ and below. However, the variable observation of dead cells (*i.e.* in 3
375 out of 5 experiments) at 10 mg L⁻¹ may inform about a transient state in the biofilm
376 response to bactericidal (*i.e.* biofilm-cidal) doses of NPs. In light of this, the absence of
377 visible dead cells at 100 mg L⁻¹ (certainly removed by the flow) is not a proof of unaltered
378 viability but a testimony of biofilm temporal response as supported by previous studies with
379 other chemicals (Bridier *et al.*, 2011; Skogman *et al.*, 2012; Tote *et al.*, 2010). Despite being
380 frequently reported, the direct comparison of the planktonic versus biofilm information may
381 be nevertheless rather inappropriate (*i.e.* the biofilm associated cells are differentiated from
382 the planktonic cells by reduced growth rate, up and down gene regulation, ability to show

383 coordinate behaviour and generation of extracellular polymeric matrix) (Booth *et al.*, 2011;
384 Bridier *et al.*, 2011). Considering the “worst case scenario”, disperse microcolonies were
385 visible *post* exposure to a single 24 h pulse of 100 mg L⁻¹ Ag NPs; the non-static *P. putida*
386 biofilms were therefore more tolerant to Ag NPs than the planktonic cells (Chernousova and
387 Epple, 2013; Mallevre *et al.*, 2014). In terms of morphology, the general trend of the biofilm
388 response was characterised by a decrease in biofilm biomass, thickness and surface area
389 coupled with an important gain in roughness. The response was found dose dependent with
390 impacts reported from 0.01 mg L⁻¹; therefore corroborating the sloughing phenomena
391 reported *post* exposure to 0.02 - 2 mg L⁻¹ Ag NPs elsewhere (Fabrega *et al.*, 2009). In
392 addition here, the microbial activity (*i.e.* monitored *via* the sole carbon source utilisation)
393 was concomitantly shown to be time dependent (*i.e.* older and larger biofilms using more D-
394 glucose in absence of NPs) as well as NP dose dependent (*i.e.* the utilisation of D-glucose
395 being reduced *post* exposure to 10 mg L⁻¹ Ag NPs and above). Consequently, the dose
396 dependent biofilm restructuring previously mentioned did not involve an evident loss in the
397 biofilm activity with the lowest concentrations of NPs (*i.e.* 0.01 - 1 mg L⁻¹ range); instead the
398 loss of activity was rather concomitant with the microbial death.

399 4.2. Potential mode of action for displayed Ag NP toxicity

400 Ag cations were reported to complex with the negatively charged extracellular matrix of the
401 biofilms, potentially diminishing their bioavailability for an eventual toxicity (Habimana *et*
402 *al.*, 2011). However, Ag ions exhibited evident dose dependent toxic effects using non-static
403 biofilms, as similarly discussed before with planktonic cultures (Losasso *et al.*, 2014;
404 Mallevre *et al.*, 2014; Notter *et al.* 2014) and static biofilms (Choi *et al.*, 2010; Radzig *et al.*,
405 2013). The occurrence of the live/dead dual staining was also visibly increased in the assays
406 in the case of the Ag ions, attesting to a superior biofilm-cidal pressure overall as previously
407 stressed by Bjarnsholt *et al.* (2007) with Ag sulfadiazine. Similar observations were also
408 reported with Zn²⁺ released ions from Zn NPs elsewhere (Hou *et al.*, 2014); the tested Ag
409 NPs were not therefore a single case example. The function, structure and extracellular
410 matrix of *P. putida* biofilms were previously discussed as impacted by the surrounding
411 nutrients (Bester *et al.*, 2011; Jahn *et al.*, 1999). The limited barrier role of the produced *P.*
412 *putida* matrix due to the minimal conditions of growth in AW may therefore be

413 hypothesised here. The tested Ag NPs were nevertheless characterised by a low (*ca.* < 5 % in
414 mass) dissolution rate elsewhere (Klein *et al.*, 2011; Mallevre *et al.*, 2014); the observed
415 impacts of NPs cannot be supported solely by the released ions thus.

416 Interest has been recently shown in investigating the NP deposition onto and penetration
417 into biofilms. Peulen and Wilkinson (2011) reported that the relative self-diffusion
418 coefficients of several NPs (including Ag NPs) were decreased exponentially with the square
419 of the NP radius when tested with *Pseudomonas* spp. static biofilms. Choi *et al.* (2010)
420 showed that Ag NPs were able to penetrate *ca.* 40 µm in static biofilms within 1 h. From a
421 non-static biofilm viewpoint, Miller *et al.* (2013) showed that distributions of NPs through
422 the biofilms were consistent with diffusive transport and that uniform distributions through
423 the thickness were achieved within a few hours. Interactions between NPs and biofilms
424 were observed herein (*i.e.* impact on UV-vis spectra, loss in concentration as well as gain in
425 size and negative charges in effluent samples) and discussed previously (Fabrega *et al.*,
426 2009). NP deposition onto and penetration into the biofilms may therefore be proposed
427 here.

428 Consequently, the observed toxicity of tested Ag NPs (*ca.* 15 nm) is likely to be supported by
429 combined NP and ion based effects. Interestingly, the dose dependant and sequential
430 impact reported on biofilm morphology, viability and activity would support the hypothesis
431 of a NP dose dependent bacteriostatic (biofilm-static) and bactericidal (biofilm-cidal) like
432 response from non-static biofilms as previously suggested with static biofilms (Choi *et al.*,
433 2010; Dror Ehre *et al.*, 2010; Inbakandan *et al.*, 2013; Martinez-Gutierrez *et al.*, 2013; Radzig
434 *et al.*, 2013; Raftery *et al.*, 2014). This would corroborate as well the notion of biofilm
435 adaptive stress response already described with other toxicants such as disinfectants
436 (Bridier *et al.*, 2011).

437 4.3. Long term effects

438 The importance of information regarding the long term effects of NPs was recently
439 emphasised (Fabrega *et al.*, 2009; Handy *et al.*, 2012). Nevertheless, such results using
440 biofilms are still to be reported in nano(ecotoxicology).

441 Herein, results from *P. putida* biofilms assessed 24 h *post* exposure to a single pulse of Ag
442 NPs/ions showed overall recovering patterns on biofilm morphology and activity. In the
443 absence of toxic pressure (*i.e.* the absence of NPs within the system during the recovery
444 period was confirmed by AAS), biofilms were shown to restructure (*i.e.* presence of
445 filaments and re-growth of microcolonies).

446 The formation of filaments by *P. putida* has been previously reported as an adaptive survival
447 strategy in response to hostile conditions of growth (Crabbe *et al.*, 2012; Jensen and
448 Woolfolk, 1985). In fact, filament formation is a typical stress response to sub-lethal
449 conditions displayed by a wide number of bacteria genera including *Escherichia coli*, *Listeria*
450 *monocytogenes* and *Bacillus cereus* (Jones *et al.*, 2013). It has been specifically reported in
451 cases of pH, pressure and temperature stresses, of low water activity or high CO₂ conditions,
452 and of antimicrobials presence (*e.g.* antibacterial peptides and disinfectants), however, we
453 believe this is the first report of biofilm related filament formation in response to Ag NP
454 stress conditions. Mechanisms of filament formation are commonly attributed to blockages
455 in the early steps of the bacterial cell division due to a reduced energy state of the cell,
456 mechanisms which were shown to be reversible (Jones *et al.*, 2013). The formation of
457 elongated bacteria was equally reported as a typical consequence of DNA damage and
458 envelope stress (Justice *et al.*, 2008). Interestingly, filaments were apparent only at 0.01 and
459 0.1 mg L⁻¹ Ag NPs here, supporting the theory that filament formation is a dose dependent
460 and reversible response as has been shown with other antimicrobial agents. We may in
461 addition postulate that other filament producing bacteria (*e.g.* *Escherichia coli*, *Listeria*
462 *monocytogenes* and *Bacillus cereus*) may similarly respond to Ag NPs under the same
463 conditions.

464 Finally, variable results and potentially late effects were observed at 96 h *post* exposure to 1
465 mg L⁻¹. Accordingly to the NP mode of action afore hypothesised, some intermediate or
466 threshold concentrations of NPs may then constitute a particularly “grey area” where mono-
467 species biofilms display heterogeneous structure due to differing responses expressed at
468 the single cell level.

469 4.4. Environmental relevance

470 The environmental concentration of NPs has been appraised around the $\mu\text{g L}^{-1}$ range in
471 surface waters and effluent wastewaters (Gottschalk *et al.*, 2013). Despite morphological
472 impacts being found from 0.01 mg L^{-1} , we demonstrated overall that biofilms exposed to
473 pristine Ag NPs (up to 100 mg L^{-1}) were capable of morphological recovery within only 24 h.
474 The microbial activity was not found significantly affected below 1 mg L^{-1} and was also
475 subjected to recovery otherwise. In addition, Ag was shown sulphidised and interacting with
476 organic matters in natural waters (Kaegi *et al.*, 2013; Levard *et al.*, 2012). We have shown
477 that Ag NPs were less toxic and more subject to aggregation, especially with ageing, in real
478 wastewaters than in artificial wastewaters (unpublished data). In light of this, the eventual
479 impacts of released and aged Ag NPs in the $\mu\text{g L}^{-1}$ range to *P. putida* biofilms may be
480 therefore limited at the present time. Additional studies using other models would be
481 necessary to extend the trends herein reported to natural biofilms.

482 The biofilm activity assessment was piloted herein using a D-glucose based monitoring. As
483 the sole carbon source of the system, D-glucose utilisation appeared as a critical marker of
484 the biofilm behaviour. Considering there is 1.07 mg of Chemical Oxygen Demand (COD) *per*
485 mg of D-glucose, the theoretical COD removal activity may be estimated too. Being quicker,
486 less sample consuming and easier to perform than the COD quantification; the D-glucose
487 monitoring was preferred across conditions and experiments. Based on the original loading
488 of D-glucose (0.5% , w/v), ecotoxicity assays were performed in AW with an equivalent COD
489 loading of *ca.* 5000 mg L^{-1} , corresponding to a high concentration case scenario. The use of
490 D-glucose (in the 0.5% range, w/v) was reported before (Bjarnsholt *et al.*, 2007; Fabrega *et*
491 *al.*, 2009; Halan *et al.*, 2011) in a similar AB trace minimal medium, minimal Davis medium
492 or M9 medium. Fabrega *et al.* (2009) also worked, in addition, in the absence/presence (up
493 to 10 mg L^{-1}) of humic substances. However, the correlation to C source utilisation or COD
494 information was not considered in any of these studies. Additional assays related to the
495 microbial activity (*e.g.* phosphorus or ammonium removal) may be anticipated for future
496 works.

497 Although well described and still improving (Crusz *et al.*, 2012; Weiss Nielsen *et al.*, 2011;
498 this work), microfluidics systems as used here may still appear difficult to assemble and
499 perform. A plethora of short term or long term as well as single and multiple pulse based

500 scenario with various NPs along with ageing and recovery assessment could be nonetheless
501 piloted in order to help better mimic possible natural events and therefore better
502 understand the real risk of NPs. At the present time though, there are scarce applications in
503 nano(ecotoxicology) with non-static mono-species biofilms (Fabrega *et al.*, 2009; this work)
504 and simply none with multi-species. Mix communities based non-static biofilms studies are
505 consequently anticipated as future critical works in nano(ecotoxicology).

506 **5. Conclusions**

507 This paper reports for the first time on the temporal assessment of Ag NP and ion impact to
508 the dynamics of mature *P. putida* based mono-species biofilms in parallelised flow-cells
509 considering biofilm morphology, viability and activity related information.

510 Short term studies showed sequential dose dependent toxic effects of Ag NPs on *P. putida*
511 biofilm morphology (with impacts characterised from 0.01 mg L⁻¹), then activity (from 1 - 10
512 mg L⁻¹ range) and viability (from 10 mg L⁻¹) *via* a single pulse of 24 h in AW. Long term effects
513 showed sequential dose dependant recovery of biofilm morphology and activity. Ag ions
514 showed dose dependent impacts too but led to more efficient recovery *post* exposure
515 despite being at least ten times more toxic than the tested Ag NPs. In lights of this and of
516 the NP characterisation information, the combined effect of NPs and ions was proposed to
517 support the observed toxicity results of tested Ag NPs.

518 Additional works using non-static biofilms are desirable in nano(ecotoxicology). Further
519 studies on multi-species biofilms along with metabolomics, communities and extracellular
520 matrix based temporal investigations are encouraged.

521 **Acknowledgements**

522 We would like to thank Heriot-Watt University (Edinburgh, UK) for providing FM with a
523 James-Watt scholarship (Heriot-Watt University, Edinburgh, UK). We thank Dr C. Sternberg
524 and Dr A. Heydorn (DTU, Lyngby, Denmark) for providing advice along with the COMSTAT 1
525 program. We acknowledge as well the European Union's Seventh Framework Programme
526 [FP7 2007-2013] under EC-GA No. 263215 'MARINA', for the provision of the Ag NPs used in
527 this study.

528 **References**

- 529 Bester, E., Kroukamp, O., Hausner, M., Edwards, E.A., Wolfaardt, G.M., 2011. Biofilm form
530 and function: carbon availability affects biofilm architecture, metabolic activity and
531 planktonic cell yield. *Journal of Applied Microbiology* 110, 387-398. DOI: 10.1111/j.1365-
532 2672.2010.04894.x.
- 533 Bjarnsholt, T., Kirketerp-Moller, K., Kristiansen, S., Phipps, R., Nielsen, A.K., Jensen, P.O.,
534 Hoiby, N., Givskov, M., 2007. Silver against *Pseudomonas aeruginosa* biofilms. *APMIS* 115,
535 921-928. DOI: 10.1111/j.1600-0463.2007.apm_646.x.
- 536 Booth, S.C., Workentine, M.L., Wen, J., Shaykhutdinov, R., Vogel, H.J., Ceri, H., Turner, R.J.,
537 Weljie, A.M., 2011. Differences in metabolism between the biofilm and planktonic response
538 to metal stress. *Journal of Proteome Research* 10, 3190-3199. DOI: 10.1021/pr2002353.
- 539 Bridier, A., Briandet, R., Thomas, V., Dubois-Brissonnet, F., 2011. Resistance of bacterial
540 biofilms to disinfectants: a review. *Biofouling* 27, 1017-1032. DOI:
541 10.1080/08927014.2011.626899.
- 542 Buckingham-Meyer, K., Goeres, D.M., Hamilton, M.A., 2007. Comparative evaluation of
543 biofilm disinfectant efficacy tests. *Journal of Microbiological Methods* 70, 236-244. DOI:
544 10.1016/j.mimet.2007.04.010.
- 545 Chernousova, S., Epple, M., 2013. Silver as antibacterial agent: ion, nanoparticle, and metal.
546 *Angewandte Chemie International Edition* 52, 1636-1653. DOI: 10.1002/anie.201205923.
- 547 Choi, O.Y., Yu, C.P., Fernandez, G.E., Hu, Z.Q., 2010. Interactions of nanosilver with
548 *Escherichia coli* cells in planktonic and biofilm cultures. *Water Research* 44, 6095-6103. DOI:
549 10.1016/j.watres.2010.06.069.
- 550 Crabbe, A., Leroy, B., Wattiez, R., Aertsen, A., Leys, N., Cornelis, P., Van Houdt, R., 2012.
551 Differential proteomics and physiology of *Pseudomonas putida* KT2440 under filament-
552 inducing conditions. *BMC Microbiology* 12. DOI: 10.1186/1471-2180-12-282.

553 Cruzs, S.A., Popat, R., Rybtke, M.T., Camara, M., Givskov, M., Tolker-Nielsen, T., Diggle, S.P.,
554 Williams, P., 2012. Bursting the bubble on bacterial biofilms: a flow cell methodology.
555 *Biofouling* 28, 835-842. DOI: 10.1080/08927014.2012.716044.

556 Dong, X., Yang, L., 2014. Inhibitory effects of single-walled carbon nanotubes on biofilm
557 formation from *Bacillus anthracis* spores. *Biofouling* 30, 1165-1174. DOI:
558 10.1080/08927014.2014.975797.

559 Dror-Ehre, A., Adin, A., Markovich, G., Mamane, H., 2010. Control of biofilm formation in
560 water using molecularly capped silver nanoparticles. *Water Research* 44, 2601-2609. DOI:
561 10.1016/j.watres.2010.01.016.

562 Duester, L., Burkhardt, M., Gutleb, A.C., Kaegi, R., Macken, A., Meermann, B., von der
563 Kammer, F., 2014. Toward a comprehensive and realistic risk evaluation of engineered
564 nanomaterials in the urban water system. *Frontiers in chemistry* 2, 39. DOI:
565 10.3389/fchem.2014.00039.

566 Eduok, S., Martin, B., Villa, R., Nocker, A., Jefferson, B., Coulon, F., 2013. Evaluation of
567 engineered nanoparticle toxic effect on wastewater microorganisms: Current status and
568 challenges. *Ecotoxicology and Environmental Safety* 95, 1-9. DOI:
569 10.1016/j.ecoenv.2013.05.022.

570 Fabrega, J., Renshaw, J.C., Lead, J.R., 2009. Interactions of silver nanoparticles with
571 *Pseudomonas putida* biofilms. *Environmental Science & Technology* 43, 9004-9009. DOI:
572 10.1021/es901706j.

573 Fournier, E., 2001. Colorimetric quantification of carbohydrates, in: Wrolstad, R.E., Acree,
574 T.E., Decker, E.A., Penner, M.H., Reid, D.S., Schwartz, S.J., Shoemaker, C.F, Smith, D.M.,
575 Sporns, P. (Eds.), *Current Protocols in Food Analytical Chemistry*. John Wiley and Sons Inc.,
576 Unit E1.1. DOI: 10.1002/0471142913.fae0101s00.

577 Gottschalk, F., Sun, T.Y., Nowack, B., 2013. Environmental concentrations of engineered
578 nanomaterials: Review of modeling and analytical studies. *Environmental Pollution* 181, 287-
579 300. DOI: 10.1016/j.envpol.2013.06.003.

580 Habimana, O., Steenkeste, K., Fontaine-Aupart, M.-P., Bellon-Fontaine, M.-N., Kulakauskas,
581 S., Briandet, R., 2011. Diffusion of nanoparticles in biofilms is altered by bacterial cell wall
582 hydrophobicity. *Applied and Environmental Microbiology* 77, 367-368. DOI:
583 10.1128/AEM.02163-10.

584 Halan, B., Schmid, A., Buehler, K., 2011. Real-time solvent tolerance analysis of
585 *Pseudomonas* sp. strain LB120ΔC catalytic biofilms. *Applied and Environmental Microbiology*
586 77, 1563-1571. DOI: 10.1128/AEM.02498-10.

587 Hall-Stoodley, L., Costerton, J.W., Stoodley, P., 2004. Bacterial biofilms: From the natural
588 environment to infectious diseases. *Nature Reviews Microbiology* 2, 95-108. DOI:
589 10.1038/nrmicro821.

590 Handy, R.D., van den Brink, N., Chappell, M., Muehling, M., Behra, R., Dusinska, M.,
591 Simpson, P., Ahtiainen, J., Jha, A.N., Seiter, J., Bednar, A., Kennedy, A., Fernandes, T.F.,
592 Riediker, M., 2012. Practical considerations for conducting ecotoxicity test methods with
593 manufactured nanomaterials: what have we learnt so far? *Ecotoxicology* 21, 933-972. DOI:
594 10.1007/s10646-012-0862-y.

595 Heydorn, A., Nielsen, A.T., Hentzer, M., Sternberg, C., Givskov, M., Ersboll, B.K., Molin, S.,
596 2000. Quantification of biofilm structures by the novel computer program COMSTAT.
597 *Microbiology* 146, 2395-2407. DOI: 10.1099/00221287-146-10-2395.

598 Holden, P.A., Schimel, J.P., Godwin, H.A., 2014. Five reasons to use bacteria when assessing
599 manufactured nanomaterial environmental hazards and fates. *Current Opinion in*
600 *Biotechnology* 27, 73-78. DOI: 10.1016/j.copbio.2013.11.008.

601 Hou, J., Miao, L., Wang, C., Wang, P., Ao, Y., Qian, J., Dai, S., 2014. Inhibitory effects of ZnO
602 nanoparticles on aerobic wastewater biofilms from oxygen concentration profiles
603 determined by microelectrodes. *Journal of Hazardous Materials* 276, 164-170. DOI:
604 10.1016/j.jhazmat.2014.04.048.

605 Inbakandan, D., Kumar, C., Abraham, L.S., Kirubakaran, R., Venkatesan, R., Khan, S.A., 2013.
606 Silver nanoparticles with anti microfouling effect: A study against marine biofilm forming

607 bacteria. *Colloids and Surfaces B-Biointerfaces* 111, 636-643. DOI:
608 10.1016/j.colsurfb.2013.06.048.

609 Jahn, A., Griebe, T., Nielsen, P.H., 1999. Composition of *Pseudomonas putida* biofilms:
610 Accumulation of protein in the biofilm matrix. *Biofouling* 14, 49-57. DOI:
611 10.1080/08927019909378396.

612 Jensen, R.H., Woolfolk, C.A., 1985. Formation of filaments by *Pseudomonas putida*. *Applied*
613 *and Environmental Microbiology* 50, 364-372. DOI: 0099-2240/85/080364-09\$02.00/0.

614 Jones, T.H., Vail, K.M., McMullen, L.M., 2013. Filament formation by foodborne bacteria
615 under sublethal stress. *International Journal of Food Microbiology* 165, 2, 97-110. DOI:
616 10.1016/j.ijfoodmicro.2013.05.001.

617 Ju-Nam, Y., Lead, J.R., 2008. Manufactured nanoparticles: An overview of their chemistry,
618 interactions and potential environmental implications. *Science of the Total Environment*
619 400, 396-414. DOI: 10.1016/j.scitotenv.2008.06.042.

620 Justice, S.S., Hunstad, D.A., Cegelski, L., Hultgren, S.J., 2008. Morphological plasticity as a
621 bacterial survival strategy. *Nature Reviews Microbiology* 6, 162-168. DOI:
622 10.1038/nrmicro1820.

623 Kaegi, R., Voegelin, A., Ort, C., Sinnet, B., Thalmann, B., Krismer, J., Hagendorfer, H.,
624 Elumelu, M., Mueller, E., 2013. Fate and transformation of silver nanoparticles in urban
625 wastewater systems. *Water Research* 47, 3866-3877. DOI: 10.1016/j.watres.2012.11.060.

626 Kahru, A., Ivask, A., 2013. Mapping the dawn of nanoecotoxicological research. *Accounts of*
627 *Chemical Research* 46, 823-833. DOI: 10.1021/ar3000212.

628 Klein, C., Comero, S., Stahlmecke, B., Romazanov, J., Kuhlbusch, T., van Doren, E., Wick, P.,
629 Locoro, G., Koerdel, W., Gawlik, B., Mast, J., Krug, H. F., Hund-Rinke, K., Friedrichs, S., Maier,
630 G., Werner, J., Linsinger, T., 2011. NM-300 silver characterisation, stability, homogeneity.
631 EUR – Scientific and Toxicological Sciences, Technical Research Reports, JRC Publication No.
632 JRC60709, EUR 24693 EN, Publications Office of the European Union. DOI: 10.2788/23079.

633 Levard, C., Hotze, E.M., Lowry, G.V., Brown, G.E., 2012. Environmental transformations of
634 silver nanoparticles: Impact on stability and toxicity. *Environmental Science & Technology*
635 46, 6900-6914. DOI: 10.1021/es2037405.

636 Losasso, C., Belluco, S., Cibir, V., Zavagnin, P., Micetic, I., Gallochio, F., Zanella, M., Bregoli,
637 L., Biancotto, G., Ricci, A., 2014. Antibacterial activity of silver nanoparticles: Sensitivity of
638 different *Salmonella* serovars. *Frontiers in Microbiology* 5. DOI: 10.3389/fmicb.2014.00227.

639 Malleve, F., Fernandes, T.F., Aspray, T.J., 2014. Silver, zinc oxide and titanium dioxide
640 nanoparticle ecotoxicity to bioluminescent *Pseudomonas putida* in laboratory medium and
641 artificial wastewater. *Environmental Pollution* 195, 218-225. DOI:
642 10.1016/j.envpol.2014.09.002.

643 Martinez-Gutierrez, F., Boegli, L., Agostinho, A., Sanchez, E.M., Bach, H., Ruiz, F., James, G.,
644 2013. Anti-biofilm activity of silver nanoparticles against different microorganisms.
645 *Biofouling* 29, 651-660. DOI: 10.1080/08927014.2013.794225.

646 Miller, J.K., Neubig, R., Clemons, C.B., Kreider, K.L., Wilber, J.P., Young, G.W., Ditto, A.J., Yun,
647 Y.H., Milsted, A., Badawy, H.T., Panzner, M.J., Youngs, W.J., Cannon, C.L., 2013. Nanoparticle
648 deposition onto biofilms. *Annals of Biomedical Engineering* 41, 53-67. DOI: 10.1007/s10439-
649 012-0626-0.

650 Morones, J.R., Elechiguerra, J.L., Camacho, A., Holt, K., Kouri, J.B., Ramirez, J.T., Yacaman,
651 M.J., 2005. The bactericidal effect of silver nanoparticles. *Nanotechnology* 16, 2346-2353.
652 DOI: 10.1088/0957-4484/16/10/059.

653 Notter, D.A., Mitrano, D.M., Nowack, B., 2014. Are nanosized or dissolved metals more toxic
654 in the environment? A meta-analysis. *Environmental Toxicology and Chemistry* 33, 2733-
655 2739. DOI: 10.1002/etc.2732.

656 Park, H.J., Park, S., Roh, J., Kim, S., Choi, K., Yi, J., Kim, Y., Yoon, J., 2013. Biofilm-inactivating
657 activity of silver nanoparticles: A comparison with silver ions. *Journal of Industrial and*
658 *Engineering Chemistry* 19, 614-619. DOI: 10.1016/j.jiec.2012.09.013.

659 Peulen, T.O., Wilkinson, K.J., 2011. Diffusion of nanoparticles in a biofilm. *Environmental*
660 *Science & Technology* 45, 3367-3373. DOI: 10.1021/es103450g.

661 Radzig, M.A., Nadochenko, V.A., Koksharova, O.A., Kiwi, J., Lipasova, V.A., Khmel, I.A., 2013.
662 Antibacterial effects of silver nanoparticles on gram-negative bacteria: Influence on the
663 growth and biofilms formation, mechanisms of action. *Colloids and Surfaces B-Biointerfaces*
664 102, 300-306. DOI: 10.1016/j.colsurfb.2012.07.039.

665 Raftery, T.D., Kerscher, P., Hart, A.E., Saville, S.L., Qi, B., Kitchens, C.L., Mefford, O.T.,
666 McNealy, T.L., 2014. Discrete nanoparticles induce loss of *Legionella pneumophila* biofilms
667 from surfaces. *Nanotoxicology* 8, 477-484. DOI: 10.3109/17435390.2013.796537.

668 Rai, M., Birla, S., Ingle, A.P., Gupta, I., Gade, A., Abd-El Salam, K., Marcato, P.D., Duran, N.,
669 2014. Nanosilver: an inorganic nanoparticle with myriad potential applications.
670 *Nanotechnology Reviews* 3, 281-309. DOI: 10.1515/ntrev-2014-0001.

671 Skogman, M.E., Vuorela, P.M., Fallarero, A., 2012. Combining biofilm matrix measurements
672 with biomass and viability assays in susceptibility assessments of antimicrobials against
673 *Staphylococcus aureus* biofilms. *Journal of Antibiotics* 65, 453-459. DOI: 10.1038/ja.2012.49.

674 Stewart, P.S., Franklin, M.J., 2008. Physiological heterogeneity in biofilms. *Nature Reviews*
675 *Microbiology* 6, 199-210. DOI: 10.1038/nrmicro1838.

676 Tote, K., Horemans, T., Vanden Berghe, D., Maes, L., Cos, P., 2010. Inhibitory effect of
677 biocides on the viable masses and matrices of *Staphylococcus aureus* and *Pseudomonas*
678 *aeruginosa* biofilms. *Applied and Environmental Microbiology* 76, 3135-3142. DOI:
679 10.1128/AEM.02095-09.

680 Weiss Nielsen, M., Sternberg, C., Molin, S., Regenber, B., 2011. *Pseudomonas aeruginosa*
681 and *Saccharomyces cerevisiae* biofilm in flow cells. *Journal of visualized experiments: JOVE*.
682 DOI: 10.3791/2383.

683 Wiles, S., Whiteley, A.S., Philp, J.C., Bailey, M.J., 2003. Development of bespoke
684 bioluminescent reporters with the potential for in situ deployment within a phenolic-

685 remediating wastewater treatment system. *Journal of Microbiological Methods* 55, 667-677.
686 DOI: 10.1016/S0167-7012(03)00203-3.

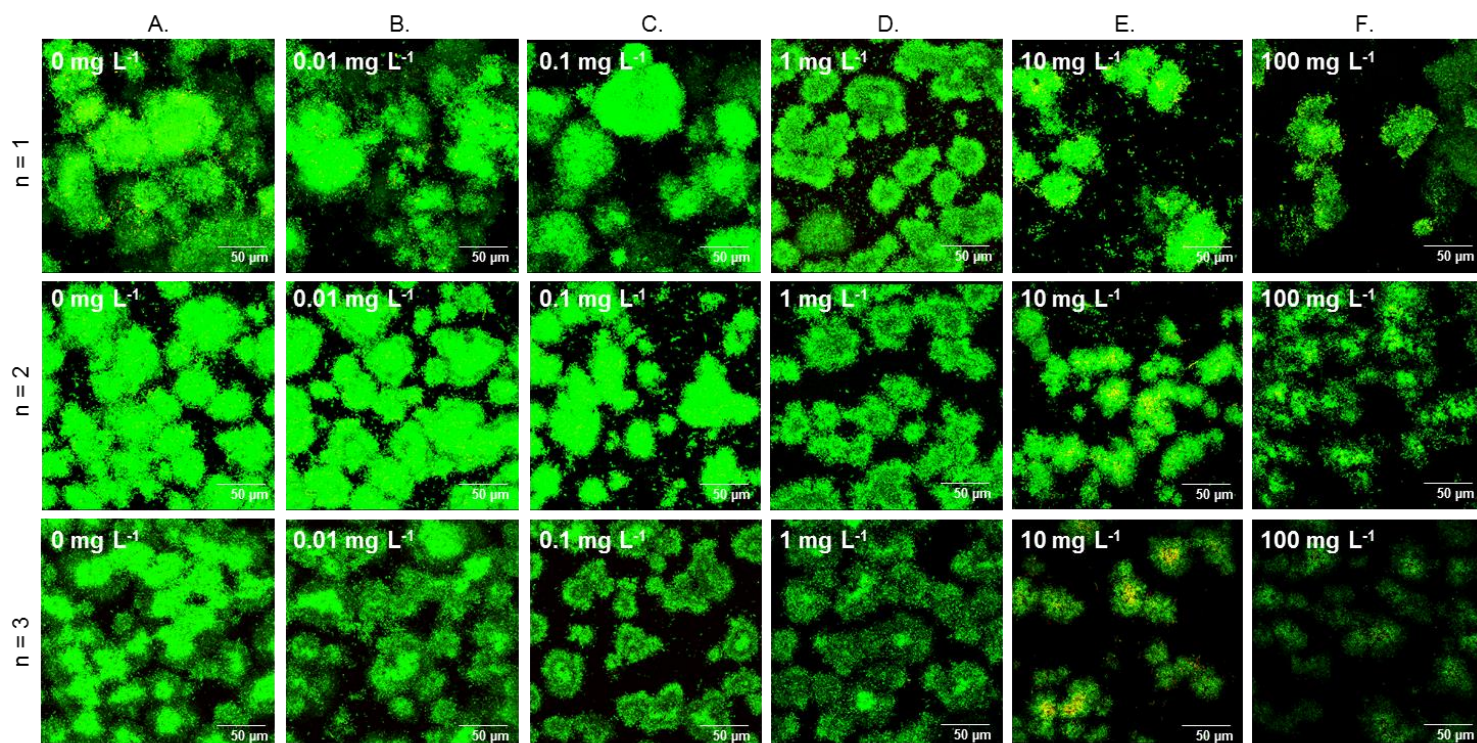
687 **Supplementary material**

688

689

690

691



692

693 **Fig. S1: Biofilm morphology characterisation *post* exposure to Ag NM-300K NPs.** Additional
694 examples of result at 72 h (*i.e. post* exposure) from three replicate experiments are presented above
695 as support for the Figure 2 (bottom row), therefore the same caption applies.

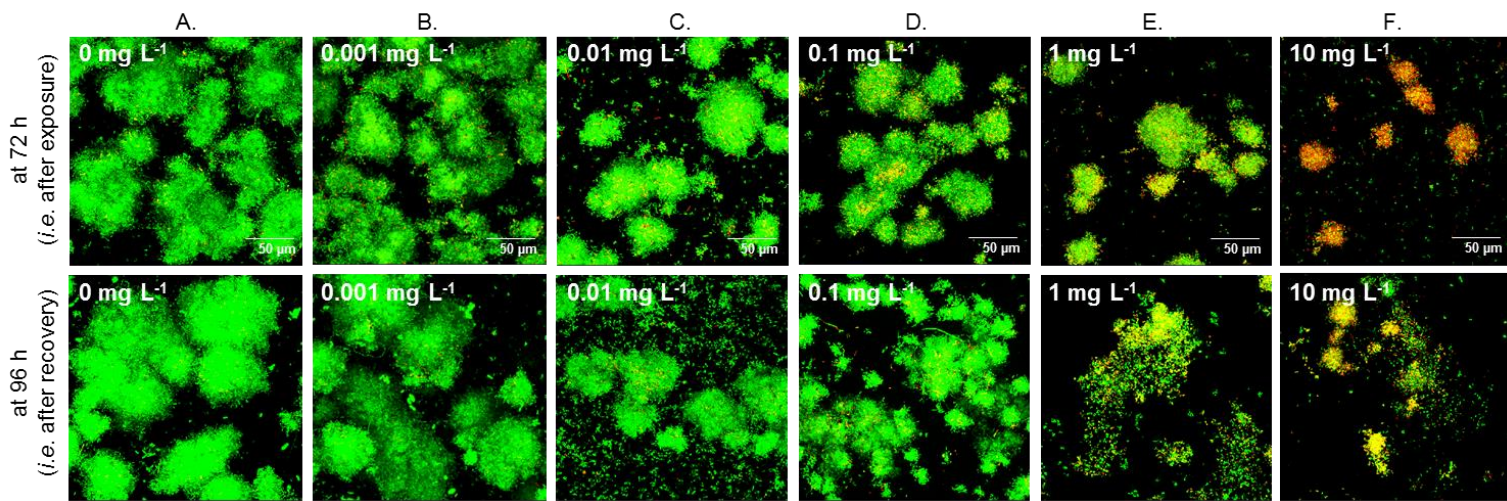
696

697

698

699

700
701
702
703
704



705

706 **Fig. S2: Biofilm morphology characterisation post exposure to Ag ions.** *Pseudomonas putida* mono-
707 species biofilms were cultured in artificial wastewater in CLSM compatible flow-cells for 48 h then
708 exposed to 0, 0.001, 0.01, 0.1, 1 and 10 mg L⁻¹ of Ag ions for 24 h (from A to F respectively). Biofilms
709 were analysed by CLSM after live/dead staining at 72 h (*i.e. ante* exposure, top row) and at 96 h (*i.e.*
710 *post* recovery, bottom row). Representative examples of maximised z-stack are shown. Each image
711 represents 1 out of 7 z-stacks randomly registered *per* condition for 1 experiment (n = 3). Scale is 50
712 µm wide.

713
714
715
716

717
718
719
720
721
722
723
724
725
726
727
728
729
730
731
732
733
734
735
736
737
738
739

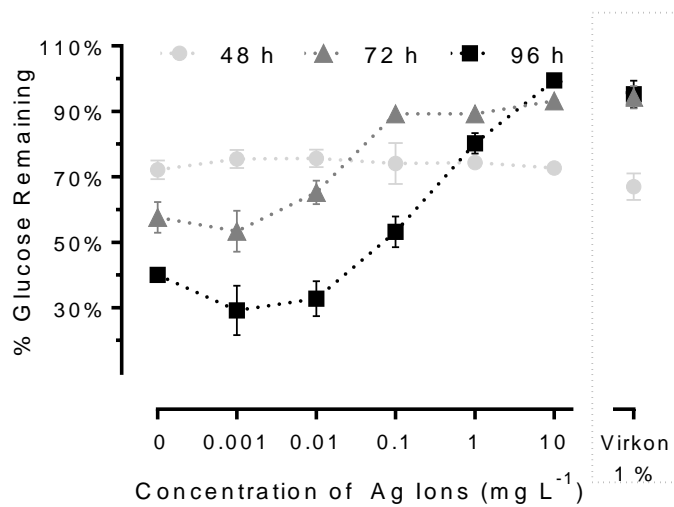


Fig. S3: Quantitative characterisation of the microbial activity (Ag ion case). Samples collected upstream (*i.e.* in influents) and downstream (*i.e.* in effluents) of the flow-cells at 48, 72 and 96 h were used for D-glucose quantification *via* the phenol - sulphuric acid assay. Presented data are mean \pm SEM (n = 3) of the calculated percentages of D-glucose remaining (in % terms) in effluents *per* tested condition. The detailed findings from the statistical analysis *via* multiple t-tests (corrected with the Holm-Sidak method) considering two parameters at a time are shown in Figure S4.

740
741
742
743
744
745
746
747
748
749
750
751
752
753
754
755
756
757
758
759
760
761
762

	48 h vs 72 h	72 h vs 96 h	48 h vs 96 h
0 mg L ⁻¹	**↗	**↗	**↗
0.01 (0.001) mg L ⁻¹	**↗ (**↗)	NSD (*↗)	**↗ (**↗)
0.1 (0.01) mg L ⁻¹	*↗ (*↗)	NSD (**↗)	**↗ (**↗)
1 (0.1) mg L ⁻¹	*↗ (*↘)	NSD (**↗)	**↗ (*↗)
10 (1) mg L ⁻¹	NSD (**↘)	NSD (*↗)	NSD (NSD)
100 (10) mg L ⁻¹	**↘ (**↘)	NSD (NSD)	NSD (**↘)
Virkon 1 %	**↘	NSD	**↘

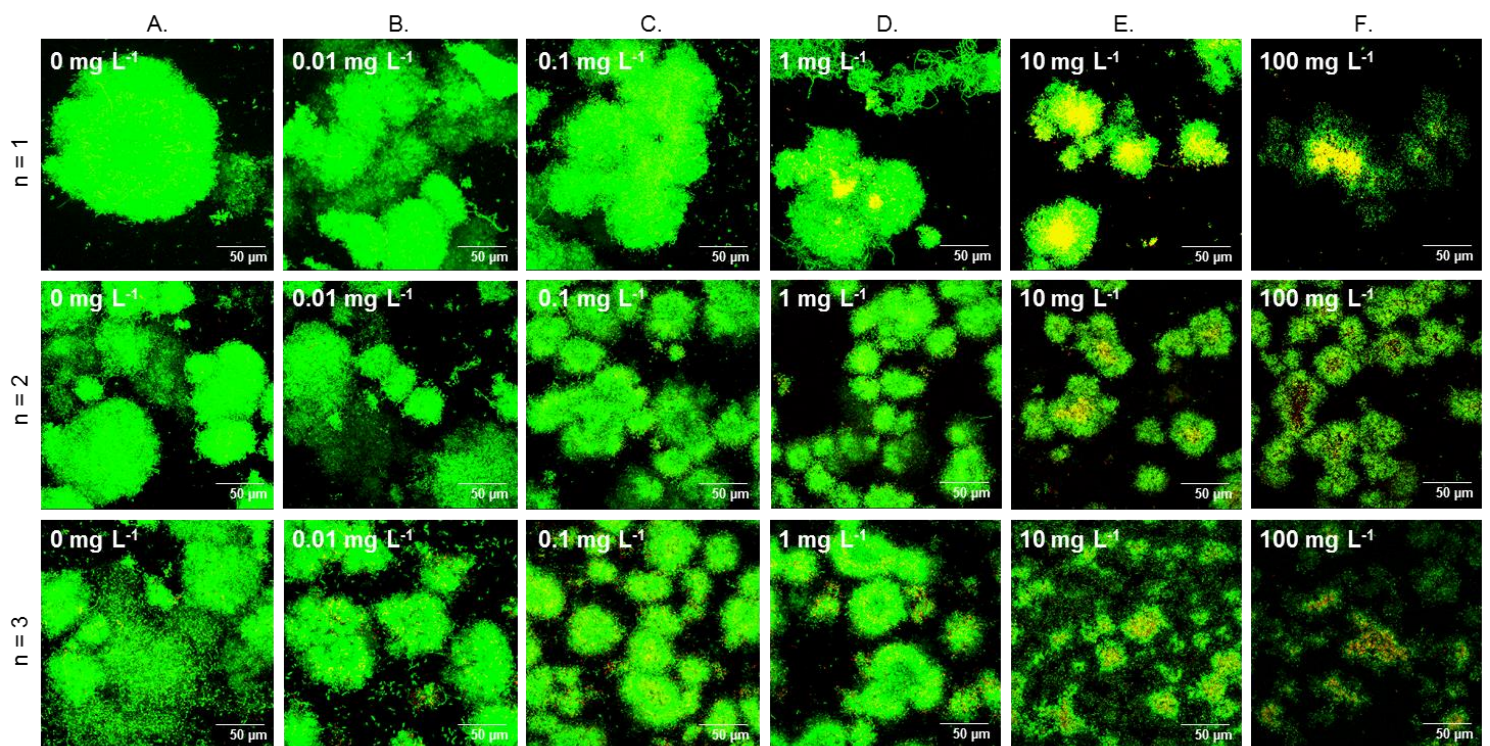
Fig. S4: Statistical analysis of the reported microbial activity results. The output results from the statistical analysis *via* multiple t-tests (corrected with the Holm-Sidak method) considering two parameters at a time are shown. The NP case is reported in blue, the ion case in red. Significantly different between time points (increased or decreased activity over time) with a *p* value < 0.1 (*) or < 0.05 (**). Non-significantly different (NSD).

763

764

765

766



767

768 **Fig. S5: Biofilm recovery assessment *post* exposure to Ag NM-300K NPs.** Supplementary examples
769 of result at 96 h (*i.e. post* recovery) from three replicate experiments are presented above as
770 support for the Figure 5, therefore the same caption applies.